Transactions of the Materials Research Society of Japan 29[4] 1709-1712 (2004)

Magnetic property enhancement of nanocrystalline $Pr_2Fe_{23}B_3$ melt-spun ribbons by refractory elements substitution

H. W. Chang, C. H. Chiu, and W. C. Chang
Department of Physics, National Chung Cheng University, Ming-Hsiung, Chia-Yi, Taiwan, R. O. C.
Fax: 886-5-2721091, e-mail: phywcc@ccu.edu.tw

The phase evolution and magnetic properties of nanocrystalline $Pr_2Fe_{23}B_3$ and $Pr_2(Fe_{0.975}M_{0.025})_{23}B_3$ (M = Nb, Ti, V and Zr) melt-spun ribbons have been investigated. For $Pr_2Fe_{23}B_3$ alloy spun at 25 m/s, a large amount of metastable $Pr_2Fe_{23}B_3$ phase is found at the as-spun state and the condition of low temperature annealing (T_H<700 °C). The magnetically hard $Pr_2Fe_{14}B$ and soft Fe_3B phase start to appear by the dissociation of $Pr_2Fe_{23}B_3$ phase at the condition of high temperature annealing (T_H≥700 °C). Two phases merely, namely, $Pr_2Fe_{14}B$ and α-Fe, can coexist only at T_H≥800 °C which enlarges the grain sizes (~80 nm) apparently and results in extremely low B_r and $_iH_c$ values of the ribbons. A slight substitution of refraction elements (i.e. Nb, Ti, V and Zr) for Fe in $Pr_2(Fe_{0.975}M_{0.025})_{23}B_3$ not only can suppress the formation of metastable $Pr_2Fe_{23}B_3$ phase but also lead to the presence of large amount of $Pr_2Fe_{14}B$ and α-Fe phases of fine grain sizes in the matrix even at lower annealing temperature (T_H≤650 °C). Among the selected refractory elements, Ti is the best candidate for magnetic enhancement of $Pr_2Fe_{23}B_3$ melt-spun ribbons. B_r = 9.9 kG, $_iH_c$= 5.7 kOe and $(BH)_{max}$ = 15.0 MGOe are obtained in $Pr_2(Fe_{0.975}Ti_{0.025})_{23}B_3$.

Key words: Nanocomposites; Melt spinning; $Pr_2Fe_{23}B_3$

1. INTRODUCTION

It is well known that two types of melt-spun nanocomposites, namely α-Fe/$Nd_2Fe_{14}B$ [1-2] and Fe_3B/$Nd_2Fe_{14}B$ [3-4], with excellent remanence B_r and maximum energy product $(BH)_{max}$ have been investigated extensively for making bonded magnets. The efforts were mostly devoted to ribbons with either low boron concentrations (~ 5-9 at %) [5] or extreme high boron concentrations (~16-20 at%) [6]. One deficiency of these types of nanocomposites is their lower coercivity ($_iH_c$ < 8 kOe) resulting from the existence of considerable amount of magnetically soft phases α-Fe or Fe_3B, which limits their applications at higher temperature (T > 100 °C).

The coercivity of the nanocomposite ribbons has been improved without the degradation of the energy product [7-9]. For instance, B_r, $_iH_c$ and $(BH)_{max}$ values of 8.6 to 9.7 kG, 9.5 to 13 kOe and of 16 to 18 MGOe, respectively, can be obtained on the boron enriched $(Nd_{0.95}La_{0.05})_{9.5-11}Fe_{bal.}Cr_2B_{10}$ ribbons [7-8]. Similarly, B_r, $_iH_c$ and $(BH)_{max}$ values of 8.4 to 9.6 kG, 9.5 to 14.3 kOe and $(BH)_{max}$ of 13.4 to 16.2 MGOe, respectively, can also be achieved on the ternary $Pr_{9.5-11.76}Fe_{bal.}B_{10}$ ribbons [9]. Trials have been made to improve the B_r and $(BH)_{max}$ values of materials in this composition region (boron of approximately 10 at%). One is to refine the average grain sizes and phase distributions by refractory elements substitution to strengthen the exchange coupling between the magnetically soft and hard grains. The alternative way could be to decrease the rare earth content from 11 to 8 at% in attempts to increase the volume fraction of the soft phase to enhance the B_r and $(BH)_{max}$ assuming reasonably high $_iH_c$ values can be retained. Unfortunately, when the rare earth content is lowered to below 9 at% and at boron concentration of around 10-11.5 at % , the metastable $R_2Fe_{23}B_3$ phase appears, with the reduction of the volume fraction of $R_2Fe_{14}B$, and deteriorates the magnetic properties drastically [10].

To date, limited reports are available dealing with the phase content and magnetic properties of melt spun ribbons of the nominal composition of $R_2Fe_{23}B_3$ (or $R_{7.14}Fe_{82.14}B_{10.72}$) [11-13]. Moreover, permanent magnetic properties reported to date are all about the negative aspects and with limited understanding regarding this metastable phase. Thus, it is important to understand the phases transformation of the $R_2Fe_{23}B_3$ prepared by melt spinning and with subsequent annealing treatments. Most importantly, how to convert the metastable $R_2Fe_{23}B_3$ phase into stable composites consisting of magnetically hard $R_2Fe_{14}B$ and magnetically soft phase is worth investigating in order to enhance the maximum energy product.

In this paper, we adopt various refractory elements (i.e. M = Nb, Ti, V and Zr) to substitute for Fe in $Pr_2(Fe_{0.975}M_{0.025})_{23}B_3$ for melt spinning in attempts to compare the phases and magnetic properties with those of the ternary $Pr_2Fe_{23}B_3$ ribbons.

2. EXPERIMENTAL

Alloy ingots with nominal compositions of

$Pr_2(Fe_{0.975}, M_{0.025})_{23}B_3$ (M = Nb, Ti, V and Zr) were prepared by vacuum induction melting. Ingot pieces were crushed into small pieces to accommodate the size of crucible for melt spinning. Melt-spun ribbons were produced from ingots with wheel speeds ranging from 13 to 25 m/s. Selected ribbons were annealed at 600-800 °C for 10 minutes to optimize crystallization and to improve the permanent magnetic properties. Phase identification and Curie temperatures of the magnetic phases were determined by a thermal gravimetric analyzer (TGA) with an externally applied magnetic field (conventionally referred as "TMA"). The magnetic properties of the ribbons were measured by a vibrating sample magnetometer (VSM). The microstructures of the ribbons are observed directly by transmission electron microscopy (TEM).

3. RESULTS AND DISCUSSION

Table 1 lists magnetic properties measured at room temperature of $Pr_2Fe_{23}B_3$ ribbons quenched at 25 m/s followed with various temperatures annealing (T_H) . At T_H = 650 °C, a B_r of 4.9 kG and $_iH_c$ of 164 Oe are obtained. With increasing T_H, both B_r and $_iH_c$ increase monotonically from 4.9 kG and 164 Oe for T_H = 600 °C to 6.7 kG and 1515 Oe for T_H = 800 °C. For $Pr_2Fe_{23}B_3$ ribbons, the optimal properties of B_r = 6.7 kG, $_iH_c$ = 1515 Oe and $(BH)_{max}$ = 1.7 MGOe are achieved when annealed at T_H = 800 °C. The ribbons with such low $_iH_c$ and $(BH)_{max}$ values are of no value for making bonded magnets.

The phase transformation of the as-spun $Pr_2Fe_{23}B_3$ ribbons undergoes many stages when annealed between 650 and 800 °C, as shown in Fig.1. Clearly, at T_H=650 °C, the amorphous precursors crystallize into a large amount of metastable $Pr_2Fe_{23}B_3$ phase with a small amount of α-Fe phase. At T_H=750 °C, the $Pr_2Fe_{14}B$ phase begins to present and coexists with α-Fe, $Pr_2Fe_{23}B_3$, and Fe_3B. At T_H =800°C, merely two phases, namely, $Pr_2Fe_{14}B$ and α-Fe, are found in the ribbons.

As noted above, magnetically soft metastable $Pr_2Fe_{23}B_3$ phase can be fully decomposed to α-Fe and $Pr_2Fe_{14}B$ by annealing the ribbons at temperature of above 800 °C. However, grain growth arose from high temperature annealing is so excessive, about 80 nm for T_H=800 °C, and diminishes the exchange-coupling effect between magnetically soft and hard grains. This explains why the magnetic properties of the $Pr_2Fe_{23}B_3$ ribbons annealed at 800 °C contains only $Pr_2Fe_{14}B$ and α-Fe phases are so poor. It is essential to find alternative method to suppress the formation of $Pr_2Fe_{23}B_3$ phase and to maintain the fine grain size simultaneously. For this reason, the refractory elements (Nb, Ti, V and Zr) were selected to substitute for Fe in the stoichiometric $Pr_2Fe_{23}B_3$.

Table II lists B_r, $_iH_c$ and $(BH)_{max}$ values of melt-spun $Pr_2(Fe_{0.975}, M_{0.025})_{23}B_3$ ribbons following their optimal crystallization treatment. As shown previously, extremely low magnetic properties of B_r = 6.7 kG, $_iH_c$ = 1.5 kOe and $(BH)_{max}$ = 1.7 MGOe are obtained in $Pr_2Fe_{23}B_3$ ribbons. However, a slight substitution of the selected refractory elements (Nb, Ti, V and Zr) for Fe in $Pr_2(Fe_{0.975}M_{0.025})_{23}B_3$ enhances magnetic properties remarkably. It is clear that Ti and V-substituted nanocomposites are most effective in enhancing B_r and $_iH_c$, respectively, in the present study. The optimal magnetic properties of B_r = 9.9 kG, $_iH_c$ = 5.7 kOe and $(BH)_{max}$ = 15.0 MGOe are achieved in the $Pr_2(Fe_{0.975}Ti_{0.025})_{23}B_3$ ribbon. Due to the lower B_r value, V-substituted nanocomposites exhibits inferior $(BH)_{max}$ of 11.3 MGOe. Besides, the Nb and Zr-substituted nanocomposites show intermediate values with B_r and $_iH_c$ ranging from 9.3 to 9.2 kG, and 6.3 to 5.8 kOe, respectively. Quite importantly, the $(BH)_{max}$ of the above selected alloy ribbons is well above 11 MGOe, which reflects the beneficial effect of refractory elements in enhancing the magnetic properties of $Pr_2Fe_{23}B_3$ melt-spun ribbons

Table I. The magnetic properties measured at room temperature of $Pr_2Fe_{23}B_3$ ribbons quenched at 25 m/s followed with various temperatures annealing.

Annealing Temperature (°C)	B_r (kG)	$_iH_c$ (Oe)	$(BH)_{max}$ (MGOe)
650	4.9	164	0
750	6.5	765	0.1
800	6.7	1515	1.7

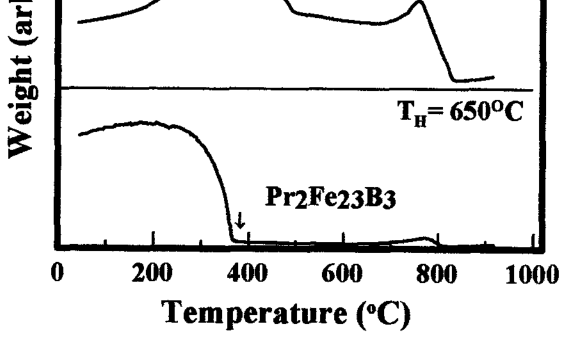

Fig. 1. TMA scans of $Pr_2Fe_{23}B_3$ ribbons quenched at 25 m/s followed with various temperatures annealing.

Shown in Fig. 2 are micrographs obtained by transmission electron microscopy of optimized ternary $Pr_2Fe_{23}B_3$ and Ti-substituted $Pr_2(Fe_{0.975}Ti_{0.025})_{23}B_3$ ribbons . Although multiple phases, namely, $Pr_2Fe_{14}B$, $Pr_2Fe_{23}B_3$, Fe_3B and α-Fe, may present in $Pr_2Fe_{23}B_3$ ribbons, it is very difficult to distinguish these phases unambiguously by TEM analysis. Nevertheless, it is clear that the average grain size of ribbons can be observed. It was estimated to be about 80-90 nm for ternary $Pr_2Fe_{23}B_3$ and 10-20 nm for M = Ti, respectively. Obviously, a slight substitution of Ti for Fe in $Pr_2(Fe_{0.975}M_{0.025})_{23}B_3$ ribbons can effectively refine grain size of the ribbons annealed at the optimal temperature (T_H= 650 °C). Same effect was also found in the ribbons with M=Nb, V and Zr.

Moreover, grain boundary phase was found to exist in $Pr_2(Fe_{0.975}Ti_{0.025})_{23}B_3$ ribbons obviously. It suggests that Ti atom may tend to react with excess boron to form Ti-boride or a solid solution in the grain boundary. As Ti atom react with excess boron to form Ti-boride in the grain boundary, the metastable $Pr_2Fe_{23}B_3$ phase diminishes or vanishes for the lack of enough boron. This explain why a slight substitution of refractory elements (i. e. Nb, Ti, V and Zr) for Fe in $Pr_2(Fe_{0.975}M_{0.025})_{23}B_3$ ribbons may suppress the formation of $Pr_2Fe_{23}B_3$ phase in $Pr_2(Fe_{0.975}M_{0.025})_{23}B_3$ melt-spun ribbons.

In summary, a slight substitution of refractory elements (Nb, Ti, V and Zr) for Fe in $Pr_2(Fe_{0.975}M_{0.025})_{23}B_3$ ribbons, incorporating a suitable annealing treatment, may suppress the formation of metastable $Pr_2Fe_{23}B_3$ phase, form maximum amount of $Pr_2Fe_{14}B$ and α-Fe, and simultaneously refine the grain size of the coexisting phases, which leads to a remarkable enhancement on the magnetic properties of $Pr_2(Fe_{0.975}M_{0.025})_{23}B_3$ ribbons.

Table II. The magnetic properties of $Pr_2(Fe_{0.975}M_{0.025})_{23}B_3$ ribbons following their optimal crystallization treatment, where M = Nb, Ti, V, and Zr.

M	Condictions		B_r (kG)	$_iH_c$ (kOe)	$(BH)_{max}$ (MGOe)
	Wheel speed (m/s)	Annealing Temperature (°C)			
--	25	800	6.7	1.5	1.7
Nb	15	700	9.3	6.3	13.6
Ti	25	650	9.9	5.7	15.0
V	13	--	8.8	6.6	11.3
Zr	25	675	9.2	5.8	12.8

According to R. Fisher et al. [14], if the average grain size was smaller than 80 nm, the exchange coupling interaction could exist either between magnetically hard phases or between hard and soft phases. Figure 3 illustrates the applied magnetic field dependence of $\delta M = m_d(H)-(1-2m_r(H))$ [15-16], with m_d being the reduced magnetization and m_r the reduced remanence, of $Pr_2(Fe_{0.975}Ti_{0.025})_{23}B_3$ ribbons after optimum annealing. The positive δM-peak height indicates the existence of exchange-coupling interaction either between magnetically hard grains or between magnetically hard and soft grains. The value of maximum δM reflects the strength of intergranular exchange coupling effect. It is clear that strong exchange coupling effect between neighboring grains existed in $Pr_2(Fe_{0.975}Ti_{0.025})_{23}B_3$ ribbons is due to their appropriate grain size and uniform distribution of grain size. Due to the effective exchange-coupling effect, higher remanence exceeding the theoretical limit for an isotropic nanocomposite ($4\pi M_s/2$) can be obtained not only in $Pr_2(Fe_{0.975}Ti_{0.025})_{23}B_3$ but also in $Pr_2(Fe_{0.975}M_{0.025})_{23}B3$ ribbons (M=Nb, V and Zr).

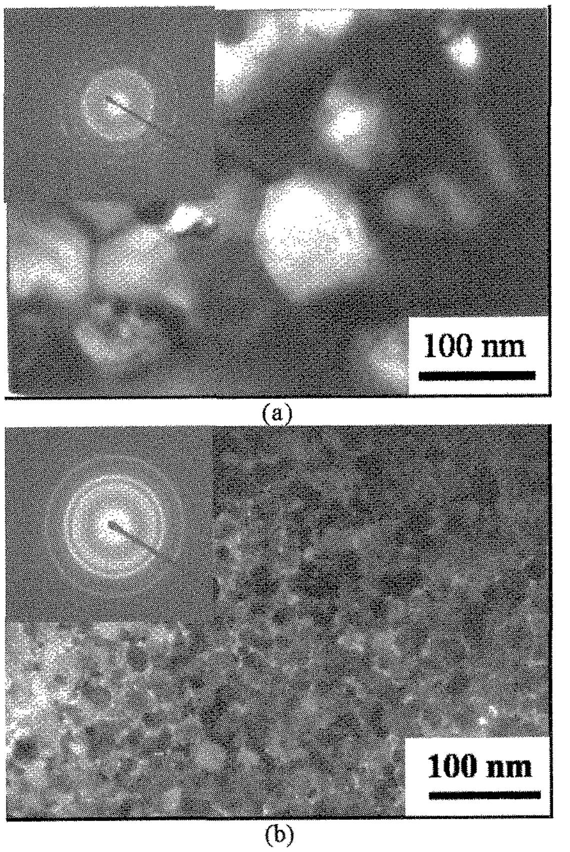

(b)

Fig. 2. TEM micrographs of (a) $Pr_2Fe_{23}B_3$ and (b) $Pr_2(Fe_{0.975}Ti_{0.025})_{23}B_3$ ribbons following their optimal crystallization treatment.

4. CONCLUSIONS

The phase evolution and magnetic properties of $Pr_2Fe_{23}B_3$ and $Pr_2(Fe_{0.975}M_{0.025})_{23}B_3$ (M = Nb, Ti, V and Zr) melt-spun ribbons have been examined. A slight substitution of the selected refraction elements (i.e. Nb, Ti, V and Zr) for Fe in $Pr_2(Fe_{0.975}M_{0.025})_{23}B_3$, incorporating a suitable annealing treatment, may suppress the formation of metastable $Pr_2Fe_{23}B_3$ phase, form maximum amount of $Pr_2Fe_{14}B$ and α-Fe, and simultaneously refine the grain size of the coexisting phases. The combination of them leads to a remarkable enhancement in the magnetic properties. The optimal magnetic properties of B_r = 9.9 kG, $_iH_c$ = 5.7 kOe and $(BH)_{max}$ = 15.0 MGOe are achieved in the $Pr_2(Fe_{0.975}Ti_{0.025})_{23}B_3$ ribbon. These magnetic properties are new record of the 2:23:3 melt-spun ribbons ever reported.

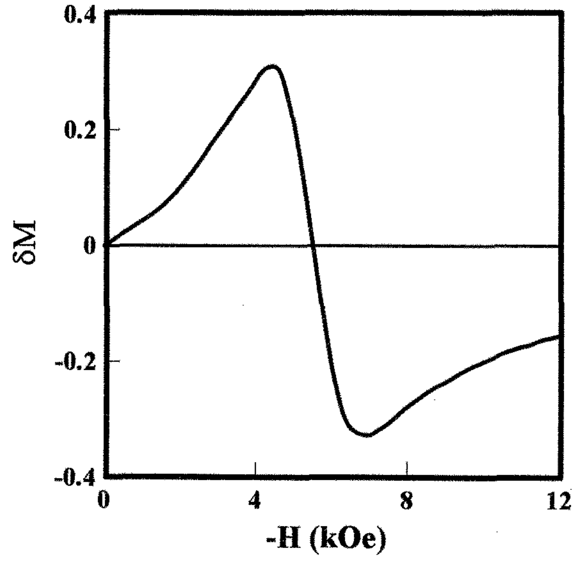

Fig. 3. The variation of δM with the externally applied magnetic field for $Pr_2(Fe_{0.975}Ti_{0.025})_{23}B_3$ ribbons following their optimal crystallization treatment.

5. ACKNOWLEDGEMENT

This paper was supported by National Science Council, Taiwan under grant no. NSC-91-2112-M-194-015.

6. REFERENCES

[1] A. Manaf, A. Buckley, H. A. Davis and M. Leonowicz, J. Magn. Magn. Mater. 101, 360 (1991).
[2] J. Bauer, M. Seeger, A. Zern and H. Kronmüller, J. Appl. Phys. 80, 1667 (1996).
[3] E. F. Kneller, R. Hawig, IEEE Trans. Magn. 27, 3588 (1991).
[4] H. Kanekiyo, M. Uehara and S. Hirosawa, IEEE Trans. Magn., 29 2863, (1993).
[5] Z. Q. Jin, Goll, H. Okumura, Y. Zhang, H. L.Wang, J. S. Munoz and G. C. Hadjipanayis, J. Magn. Magn.Mater. 248, 216 (2002).
[6] H. Kanekiyo, M. Uehara and S. Hirosawa, IEEE Trans. Magn. 29, 2863 (1993).
[7] W. C. Chang, D. Y. Chiou, S. H. Wu, B. M. Ma, Q. Chen and C. O. Bounds, J. Appl. Phys. 83, 6271 (1998).
[8] W. C. Chang, D. Y. Chiou, S. H. Wu, B. M. Ma and C. O. Bounds, Appl. Phys. Lett. 72, 121 (1998).
[9] H. W. Chang, W. C. Chang, J.C. Ho, W.M. Hikal and H.H. Hamdeh, Physica B. 327, 292 (2003).
[10] W. C. Chang, J. F. Wen, H. W. Chang, M. D. Lee and B. M. Ma, J. Magn. Magn. Mater., 239, 433(2002).
[11] B. G.. Shen, L. Y. Yang, L. Cao, H. Y. Yang, J. G. Zhao and F. M. Yang, J. Magn. Magn.Mater. 104, 1281 (1992).
[12] C. Gou, Z. X. Cheng, D. F. Chen, S. W. Niu, Q. W. Yan, P. L. Zhang, B. G.. Shen and L. Y. Yang, J. Magn. Magn.Mater. 128, 26 (1993).
[13] Zhongmin Chen, Benjamin R. Smith, Bao-Min Ma, Mei-Qing Huang, Ya-Qiao Wu and Matthew J. Kramer, IEEE Trans. Magn. (2003) in press.
[14] R. Fischer, T. Schrelf, H. Kronmüller and J. Fidler, J. Magn. Magn. Mater. 153, 35 (1996).
[15] P. E. Kelly, K. O'Grady, P. I. Mayo and R. W. Cantrell, IEEE Trans. Magn. 25, 388 (1989).
[16] F. Vajda and E. D. Torre, J. Appl. Phys. 75, 5689 (1994).

(Received October 8, 2003; Accepted February 2, 2004)